# Applications of synchrotron X-ray nano-probes in the field of cultural heritage

Marine Cotte, Anaïs Genty-Vincent, Koen Janssens, Jean Susini

C. R. Physique 19 (2018) 575–588

Contents lists available at ScienceDirect

Comptes Rendus Physique

www.sciencedirect.com

Physics and arts / Physique et arts

# Applications of synchrotron X-ray nano-probes in the field of cultural heritage

## *Application des nano-faisceaux de rayons X synchrotron dans le domaine du patrimoine*

Marine Cotte [a,b,*], Anaïs Genty-Vincent [c], Koen Janssens [d], Jean Susini [a]

[a] *European Synchrotron Radiation Facility (ESRF), BP 220, 38043 Grenoble cedex, France*
[b] *Sorbonne Université, CNRS, Laboratoire d'archéologie moléculaire et structurale (LAMS), UMR 8220, 75005 Paris, France*
[c] *Centre de recherche et de restauration des musées de France (C2RMF), Palais du Louvre, 75001 Paris, France*
[d] *Department of Chemistry, AXES Research Group, University of Antwerp, Antwerp, Belgium*

ARTICLE INFO

*Article history:*
Available online 13 August 2018

*Keywords:*
Synchrotron
Nano-probe
Cultural heritage
X-ray fluorescence
X-ray diffraction
X-ray absorption spectroscopy

*Mots-clés :*
Synchrotron
Nano-sonde
Patrimoine
Fluorescence des rayons X
Diffraction des rayons X
Spectroscopie d'absorption des rayons X

ABSTRACT

Synchrotron-based techniques are increasingly used in the field of cultural heritage, and this review focuses notably on the application of nano-beams to access high-spatial-resolution information on fragments sampled in historical or model artworks. Depending on the targeted information, various nano-analytical techniques can be applied, providing both identification and localization of the various components. More precisely, nano-X-ray fluorescence probes elements, nano-X-ray diffraction identify crystalline phases, and nano X-ray absorption spectroscopy is sensitive to speciation. Furthermore, computed tomography-based techniques can provide useful information about the morphology and in particular the porosity of materials.



RÉSUMÉ

Le domaine du patrimoine bénéficie de plus en plus des techniques utilisant le rayonnement synchrotron. Cette revue se concentre sur les nano-sondes, qui permettent des analyses précises de fragments prélevés sur des œuvres historiques ou modèles. Selon l'information souhaitée, de nombreuses techniques nano-analytiques peuvent être utilisées, donnant simultanément accès à l'identification et à la localisation des différents composants. Plus précisément, la nano-fluorescence, la nano-diffraction et la nano-spectroscopie d'absorption des rayons X sondent respectivement la composition élémentaire, les structures cristallines et la spéciation. Parallèlement, les techniques basées sur la tomographie par rayons X caractérisent la morphologie et, en particulier, la porosité des matériaux.



* Corresponding author at: European Synchrotron Radiation Facility, BP 220, 38043 Grenoble cedex, France.
*E-mail address:* cotte@esrf.fr (M. Cotte).

https://doi.org/10.1016/j.crhy.2018.07.002
1631-0705/

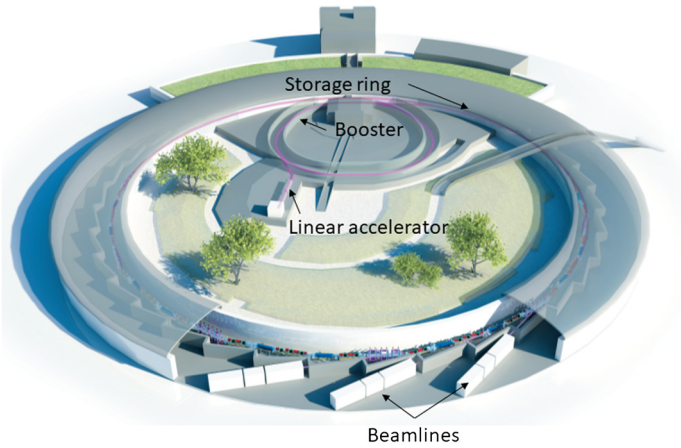


**Fig. 1.** Sketch of the ESRF.

## 1. Introduction about the synchrotron radiation and its applications in the field of cultural heritage

Within the wide range of analytical techniques applied in the field of cultural heritage, the use of synchrotron radiation-based methods has significantly increased over the last two decades. Third-generation synchrotron sources are large-scale research facilities, composed of a linear accelerator, a booster, and a storage ring (Fig. 1) [1]. These three elements produce, accelerate and store an electron beam. Upon interaction with a magnetic field, and providing they have the sufficient speed, the electrons will emit a so-called synchrotron radiation. The emission is mainly in the X-ray range; hence these sources are usually considered as (super-bright) X-ray sources. Besides, the emitted spectrum extends to the UV, visible, and infrared domains. One major characteristic of synchrotron radiation is its spectral brightness – photon flux per unit phase space volume, often given in units of photons $\cdot s^1 \cdot mrad^{-2} \cdot mm^{-2} \cdot (0.1\%\ bandwidth)^{-1}$ – which is at least 11 orders of magnitude higher than the standard laboratory X-ray sources, in particular thanks to the natural collimation of the beam. Moreover, synchrotron light offers interesting longitudinal and transversal coherence properties. By adjusting the magnetic fields interacting with the electron beam (mainly through the use of bending magnets and insertion devices), one can tailor the properties of the emitted light, in particular the spectral distribution (with an extended and tunable energy range) and the polarization. Then, the insertion in the beam of various elements such as, e.g., slits, focusing optics, mirrors, monochromators, attenuators, offers a further control of beam size, spectral distribution, and flux as well. The choice of the beam source and of these various elements will fundamentally define the characteristics of the different "beamlines" implemented tangentially to the storage ring (Fig. 1). Additionally, the choice of the detection schemes will greatly set the specificities of the beamlines. Many techniques are available at synchrotron facilities; they are based on absorption, emission, and/or scattering. These various techniques provide accurate chemical and physical information such as density, elemental composition, chemical composition, structural composition, crystallinity, morphology, optical luminescence, etc. The high flux usually translates into short acquisition times or study of species in lower concentration. This opens two main possibilities: kinetics studies of dynamic systems (through the acquisition of data on the same sample), and imaging study of (usually static) systems (through the acquisition of data at different places of a sample, as 2D or even 3D scans, when possible). In the latter case, the chemical and physical information can be not only identified, but also localized within a complex material.

Cultural heritage objects are by essence precious; accordingly, the fact that all this information can be gathered only by measuring the light-matter interactions, and with minimum sample manipulation is a major asset of these techniques. Besides, artistic and ancient objects are usually made of extremely complex and heterogeneous materials, as the result of the mixing and interactions of many constituents, and of the further evolution/degradation of the matter as well as the deposition/reaction of pollutants. Hence, the various contrasts offered by (imaging) synchrotron techniques are particularly relevant. The main synchrotron techniques used in the field of cultural heritage are X-ray fluorescence (XRF), X-ray diffraction (XRD), X-ray absorption spectroscopy (XAS), X-ray computed tomography (CT), Fourier transform infrared (FTIR) spectroscopy, and ultraviolet/visible (UV/VIS) spectroscopy [1–5]. The principles and attributes of these methods are reviewed in [1].

Back to the beam properties and applications of scanning techniques, an important aspect to be considered is the probe size. (Sub)millimetric beams can be efficiently used to scan large objects. 2D macro-XRF is becoming today a conventional laboratory technique for the analysis of paintings [6] and was pioneered at a synchrotron facility [7]; the same applies to 2D macro-XRD [8,9]. These techniques are very well suited to image chemical and physical properties at the object scale and highlight differences in the various areas of the artwork, which can be related to the use of various materials, for example for colour rendering. However, such beams are too large to distinguish heterogeneities at the micrometric scale. This scale is particularly important in the field of cultural heritage, since this is the typical thickness of the layers constituting the surface and sub-surface of the objects (being for example paint, glaze, varnish layers in paintings, sculptures, ceramics, etc.).

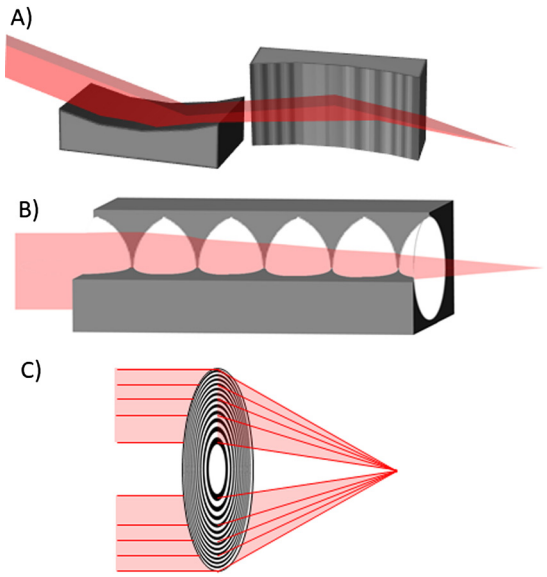


**Fig. 2.** Scheme of the three main X-ray focusing optics: (A) Kirkpatrick–Baez (KB) mirror system, (B) compound refractive lenses (CRL), and (C) Fresnel zone-plates (FZP).

For such investigations, micro- and nano-probes as developed on state-of-the-art synchrotron beamlines are particularly efficient. They are usually applied on fragments sampled in historical or model artworks. The principles and features of such synchrotron-based micro/nano analytical techniques are reviewed here, with recent examples of applications in the field of cultural heritage. In fact, most of the examples shown below have been obtained with a micrometric or sub-micrometric beam ($\geq$0.5 µm) (Table 1). The use of nanoprobes ($\leq$100 nm) is still pioneering in the field of cultural heritage and is challenging, for many reasons discussed in the last section.

## 2. The development of X-ray focusing optics

The three physical processes, refraction, diffraction and reflection, which are traditionally at the basis of the visible light optics are challenging to use in the same way to the design of X-ray lenses. The physical origin of these difficulties is closely linked to the very nature of interactions of X-rays with matter. Notably, the small deviation $\delta$ of the refractive index of condensed matter from unity makes it difficult to extend refraction-based optics from the optical spectral region to the X-ray region, because the refraction angle is proportional to $\delta$. Similarly, it is very challenging to extend diffraction-based focusing techniques to X-rays because the diffraction angle scales inversely with wavelength. Finally, the use of reflection-based optics is also limited by the very small critical angle for total reflection. Despite these fundamental limits and driven by the concomitant development of new X-ray sources, the achievable lens performances have been revolutionized by major advances in precision fabrication of mirrors and zone plates and by new concepts. A very comprehensive review can be found in [10], and the following section is concentrated to a concise and practical description of the three major types of X-ray lenses (Fig. 2).

The oldest method for micro-focusing X-rays is with mirror optics (Fig. 2A). X-ray mirrors can be either single-layer total-reflection mirrors, which reflect wide-bandpass beams at very low glancing angles, or multilayer mirrors based on Bragg diffraction with 10 to 0.1% energy bandpass at much larger angles. Most mirrors for micro/nanofocusing are today elliptical and aligned in the so-called Kirkpatrick–Baez (KB) geometry as pioneered by Kirkpatrick and Baez in the 1940s. Both mirrors can be figured either by polishing or mechanically bent into the desired elliptic shape. A major step was the ultra-smooth, near-atomic polishing methods [11,12]. Advantageous characteristics of these optics include their high reflectivity, relatively long focal length – several centimetres is typical – to accommodate specific sample environments and their inherent achromaticity, so that the incident beam energy can be tuned for spectroscopy applications without any need to adjust the focus on the specimen. For applications with high resolution and/or at high energies, best results have been obtained with multilayer coated mirrors, where the beam was focused down to sub-13-nm (FWHM) diffraction-limited X-ray focus size at 33 keV [13].

Compound refractive lenses (CRL) rely on the slight difference in refractive indices of materials compared to air (or vacuum) [14]. Since this difference is very small, single refractive lenses, for example, would have radii of only a few microns and yet give focal lengths of many meters. To make a lens system that gives shorter focal length and larger aperture, the adopted solution is a compound refractive lens, which consists of a linear array of many cylindrical concave holes of low-$Z$ materials (Fig. 2B). Fabricating CRL from low-$Z$ materials like Li, Be, B, C and Al minimizes the problems associated with absorption and allows a large number of lenses to be stacked ($N > 100$). More recently, microelectronics silicon lithography

**Table 1**
List of the main beamlines where the experiments mentioned in this article were performed.

| Country | Facility | Beamline | Techniques | Energy range (keV) | Minimum beam size or lateral resolution ($\mu m^2$, ver × hor) | Website | Publications quoted in this article |
|---|---|---|---|---|---|---|---|
| USA | ALS | 11.0.2.2 | STXM, ptychography | 0.09–2 | 0.025 × 0.025 | https://als.lbl.gov/beamlines/11-0-2/ | [55] |
| USA | ALS | 12.3.2 | XRD (white beam & monochromatic), XRF | 6–22 | 0.5 × 0.3 | https://sites.google.com/a/lbl.gov/bl12-3-2/ | [41] |
| USA | APS | Center for Nanoscale Materials Hard X-ray Nanoprobe instrument, 26-ID | XRF, XRD, ptychography | 6–12 | 0.03 × 0.03 | https://www.aps.anl.gov/Microscopy/Beamlines/26-ID | [28,29] |
| USA | SSRL | beamline 2-3 | XRF, XAS, XRD | 4.9–23 | 2 × 2 | https://www-ssrl.slac.stanford.edu/content/beam-lines/bl2-3 | [49,50,59] |
| USA | SSRL | beamline 6-2c | TXM, XRF | 2.36–17.5 | 0.2 × 0.4 | https://www-ssrl.slac.stanford.edu/content/beam-lines/bl6-2c | [58,59] |
| Canada | CLS | 10ID-1 | STXM | 0.3–10 | 0.03 × 0.03 | http://www.lightsource.ca/beamlines/details/soft_xray_spectromicroscopy_sm.html | [56,57] |
| France | ESRF | ID16A | Coherent imaging, XRF, ptychography | 17 and 33.6 | 0.03 × 0.03 | http://www.esrf.eu/UsersAndScience/Experiments/XNP/ID16A | [75–78] |
| France | ESRF | ID16B | XRF, XAS, XRD, XEOL, XBIC | 6–65 | 0.05 × 0.05 | http://www.esrf.eu/UsersAndScience/Experiments/XNP/ID16B | [52,81] |
| France | ESRF | ID21 | XRF, XAS, XRD | 2–11 | 0.3 × 0.7 | http://www.esrf.eu/id21ch | [24–26,31–34,45–47,49,51,58,59,79,80,82] |
| France | ESRF | ID19 | µCT | 10–250 | 0.1 × 0.1 | http://www.esrf.eu/home/UsersAndScience/Experiments/StructMaterials/ID19.html | [70,71] |
| France | SOLEIL | LUCIA | XRF, XAS | 0.8–8 | 2 × 2 | https://www.synchrotron-soleil.fr/fr/lignes-de-lumiere/lucia | [48] |
| Germany | Petra-III | Hard X-ray Micro/Nano-Probe beamline P06 | XRF, XAS, XRD (2D/3D), ptychography | 5–23 | 0.35 × 0.35 | http://photon-science.desy.de/facilities/petra_iii/beamlines/p06_hard_x_ray_micro_nano_probe/index_eng.html | [32,37,38,83] |
| Switzerland | SLS | PolluX | STXM | 0.25–1.6 | 0.04 × 0.04 | https://www.psi.ch/sls/pollux/pollux | [56] |
| Switzerland | SLS | TOMCAT | µCT | 8–45 | 0.16 × 0.16 | https://www.psi.ch/sls/tomcat/ | [72–74] |

fabrication technology has been applied to obtain silicon-based lenses into a composite array producing sub-100 nm hard X-ray beams. CRL is likely the most efficient X-ray focusing lens for energies exceeding 50 keV where mirrors and other lenses cannot be used. However, since CRL are chromatic, it is more difficult to use them for spectroscopic applications.

Fresnel zone-plates (FZP) are chromatic diffractive lenses (Fig. 2C) and their applications were traditionally limited to rather soft X-rays. The efficiency of a binary FZP is maximized when the structure height is tuned to introduce a phase shift of $\pi$. In the soft X-ray region, FZP efficiency is limited to about 15% due to photoelectric absorption. For X-ray energies greater than 3 keV, it is in principle possible to produce phase zone plates with focusing efficiencies close to 40%. In practice, it is difficult to manufacture thick lenses while keeping their resolution or size of the structure small [15]. For example, the appropriate zone thickness for 10 keV X-rays is estimated to be about 2 µm, even for high-density materials like gold or tantalum. The resulting extreme aspect ratios (height/width of finest zone) are the reason why FZPs for hard X-rays are more challenging. To improve the focusing efficiency, FZP with a blazed zone profile were manufactured and 55% efficiency for the nickel circular FZP at 7 keV was measured [16]. To overcome these limits, several strategies have been explored, such as stacking several thin FZPs. Finally, a recent approach proposed by Kang et al. [17] for high-resolution X-ray focusing is Multilayer Laue Lenses (MLL). MLLs represent a promising planar variation on the zone-plate approach, in which high-precision multilayer deposition techniques are used to produce relatively thick zone plates. Because a single MLL produces a line focus, crossed-pairs are needed for point nanobeams. In addition, improved focusing is achieved by titling MLLs. These high-aspect devices have already demonstrated line-focusing to 16 nm [18]. The approach is particularly well suited for high-resolution focusing optics for use at high photon energy, and a 17-nm resolution was recently reported and is now routinely integrated in X-ray microscopes [19].

## 3. Applications to cultural heritage

### *3.1. Elemental characterization at the nano scale: nano-XRF mapping*

The most popular technique for the chemical analysis of artworks at synchrotron facilities, possibly with a nano-probe, is doubtless XRF. The reasons are many. First, researchers in the field of cultural heritage are usually very familiar with gathering and interpreting elemental composition. Indeed, this fundamental characteristic of the matter can be rather easily accessed, with electron probes [20] or X-ray probes [21]. The latter can be performed with laboratory instruments, but this technique is also increasingly applied *in situ* thanks to portable devices. 2D macro-XRF analysis of paintings [6] may soon become as common as X-ray radiography. The knowledge of elemental composition is usually the first step towards the identification of the materials composing the artistic matter. As detailed in [21], this technique is beneficial for the study of all types of artistic materials (paintings, photographs, alloys, ceramics, glasses, manuscripts, etc.). Second, the success of XRF at synchrotron facilities may be related to its relatively easy implementation. This technique can be applied directly onto objects, on any material, without constraints regarding crystallinity or/and thickness of the sample/object. Data collection does not require a sophisticated set-up, which usually consists only in an energy-dispersive detector. In the 45°/45° geometry, the sample is canted 45° to the incident beam and X-ray detectors placed in the plane of the storage ring and at 90° to the incident beam. The incoming beam being naturally polarized in the horizontal plane, this geometry minimizes the contribution of elastically scattered primary X-rays. Another asset of synchrotron sources versus standard X-ray sources for XRF analyses is brightness, which translates not only into reduced dwell time, hence the possibility to acquire millions of spectra on a unique object [7], but also into lower detection limits. As an example, it can be used to quantify traces in historical glasses and thus get some insights into manufacturing technologies [22]. Finally, the SR sources also offer an extended and tunable spectral range. This leads first to the possibility of selecting the excitation energy to maximize the emission of the targeted element while minimising emission line overlaps. The second advantage, as exemplified below, consists in exciting an element of interest at a few peculiar energies (close to an absorption edge), sensitive to the speciation of this element. This way, different species containing the same elements can be mapped.

Macro-XRF (beam of a few hundreds of microns) will typically be used to map elemental distribution at the object scale and to see, for instance, if a painter used the same pigments to render all the blues, or the reds over a painting. It can also be used to reveal underpainting [23] or hidden paintings [7]. Recently, it has been applied to probe the presence of metals (lead) in the ink in Herculaneum papyri [24]. The use of µXRF (beam of a few microns) will be usually required for the study of fragments, generally prepared as cross sections, to determine the elemental composition in the different layers of a stratigraphy. This resolution is useful to probe the heterogeneity in the third dimension (perpendicular to the surface) for example to reveal the deposition of pollutants at the surface [25]. µXRF can also be used to identify possible mixtures of different constituents within the same layer and to provide insights into the way the artist combined materials: e.g., the nature and proportion of different pigments mixed in the same paint, the size of pigment particles [26]. µXRF applied to the above mentioned ink in Herculaneum papyri revealed a co-localization of Pb, P, and Cl at the micron scale, giving clues that these three elements enter the composition of a unique compound (possibly phosphohedyphane, $Ca_2Pb_3(PO_4)_3Cl$, as identified in a fine black powder found in a glassy *unguentarium* from Pompeii [27]).

The use of nano-XRF offers the possibility to further zoom-in, and probe elemental distribution at the components' scale. This can give insight about the ways they were manufactured. As an example, nano-XRF has been used to obtain highly spatially resolved and highly sensitive maps of metal impurities (in particular Pb, Cd, Fe) in submicron particles of zinc oxide pigments used in early 20th century artists' tube paints and enamel paints [28]. The analyses were carried out at

the Centre for Nanoscale Materials Hard X-ray Nanoprobe instrument, operated on ID-26 at the Advanced Photon Source, Argonne National Laboratory [29]. The beam size was focused down to 200 nm using an FZP. The objectives of the study were to compare composition (and in particular evaluate the presence of impurities) in zinc oxide paints produced by different renown paint makers (in particular Ripolin and Lefranc). Nano-XRF not only probed the presence and abundance of fillers and additional whites (based on Pb, Ti, Ca) surrounding the ZnO particles, but highlighted the presence of Fe as well within the ZnO nanoparticles, in Ripolin paints. Understanding the implication of such impurities as well as particle size and shape on the luminescence of ZnO nanoparticles would be of high interest [28].

### *3.2. Phase identification and mapping at nano-scale: 2D/3D nanoXRPD*

Complementary and/or simultaneously to XRF, XRD can be used to further identify the artistic compounds. The experimental conditions for XRD are numerous: the sample can be fixed, rotated or scanned (in 2D or 3D). It can be almost parallel to the beam (reflection geometry) or rather perpendicular (transmission geometry). The detection can be obtained with a single (or multi) element detector, rotated over an angular range; or with a 2D detector (which can also be moved to access larger angular ranges). The conditions can be such that the beam size is smaller than the crystallite size (monocrystal-type diffraction) and much larger (X-ray powder diffraction, XRPD). In the field of cultural heritage, samples are usually polycrystalline (with a possible amorphous contribution) and, if using a micro-probe, the beam size is usually much larger than the crystallites, meaning that many crystallites, randomly oriented, simultaneously diffract, leading to the so-called Debye–Scherrer rings. The primary information provided by XRPD is phase identification and determination of lattice parameters. In addition, it can also be used to characterize crystallinity (and percentage of amorphous material) [27] or dislocation and strain. These crystallographic parameters can provide a signature of the physical treatments applied to matter during manufacturing steps (e.g., crushing, annealing, sieving) [30]. XRD is particularly interesting when the elemental information is not sufficient to fully characterize material composition. As an example, “lead white” pigments have been extensively used in paintings, since the Antiquity until the 20th century. They are generally made of a mixture of cerussite $PbCO_3$ and hydrocerussite $Pb_3(CO_3)_2(OH)_2$. The presence of lead white is generally simply assessed by the detection of lead in a white pigment. However, the accurate determination of its composition and micro-structure, in particular the ratio between cerussite and hydrocerussite and the size of the crystallites can give clues about the processes followed for the preparation of the pigment (and concomitantly about the quality of the pigment). The combination of synchrotron-based high-angular-resolution and high-lateral-resolution XRD has been exploited to this purpose, to reveal the precise chemical and structural composition of fragments from 27 major paintings by old European masters dating from the 14th century to the late 19th century [31]. Similarly, XRD (with laboratory source and at SR facilities) allowed identifying different “chrome yellow” pigments in Van Gogh’s and contemporaries’ paintings. This pigment can be present as various chemical compounds ($PbCrO_4$ and $PbCr_{1-x}S_xO_4$) and various structures (orthorhombic and monoclinic) [32] which end into various colours and various photosensitivities [33]. In the two above cases, the use of a SR micro-probe allowed identifying and mapping phases in the different layers of tiny fragments. In addition to the determination of manufacturing fingerprints, μXRD can also be employed to characterize degradation compounds, impacting the aesthetical aspects of artworks. As examples, the spontaneous transformations of the red pigments vermilion (HgS) and minium (aka red lead, $Pb_3O_4$) can be mentioned here.

Vermillion (when synthetic) and cinnabar (when natural) red, red pigments used by artists in all historic periods, display both a tendency to darken/turn black and to develop white precipitates at their surface. Radepont et al. [34] and Da Pieve et al. [35] have investigated the effect of chlorinated oxidizing agents on the stability of HgS and arrived, both experimentally and theoretically, at the conclusion that HgS can gradually transform into mixed S, Cl compounds of Hg, such as corderoite ($\alpha$-$Hg_3S_2Cl_2$) and kenhsuite ($\gamma$-$Hg_3S_2Cl_2$), which in their turn can transform to (white) calomel ($Hg_2Cl_2$) and sulphates. Multilayers stacks of degradation products found on top of a strongly degraded vermillion layer in a wall painting confirmed this. A final transformation converts the calomel into soluble $HgCl_2$ and metallic Hg, considered responsible for the black colour [36]. Red lead, another semiconductor pigment used by artists since antiquity, is known to undergo several discolouration phenomena. These transformations are either described as darkening of the pigment caused by the formation of either plattnerite ($\beta$-$PbO_2$) or galena (PbS) or as whitening by which red lead is converted into anglesite ($PbSO_4$) or (hydro)cerussite. X-ray powder diffraction tomography [37] was used to investigate a microscopic paint sample from “Haystacks”, by Van Gogh. Experiments were carried out at the P06 hard X-ray micro-nano-probe beamline PETRA III, DESY, with a $0.5 \times 0.5$-$\mu m^2$ beam. They revealed that a rare lead mineral, plumbonacrite ($3PbCO_3{\cdot}Pb(OH)_2{\cdot}PbO$), was formed *in-situ*, at the interface between the original pigment grain, consisting of minimum, and the degradation products that formed on its surface (see Fig. 3). The possibility of XRPD tomography to visualize the internal distribution of different crystalline compounds in complex samples was exploited here. Plumbonacrite constitutes the missing link between, on the one hand, the photo-induced reduction of red lead and, on the other hand, (hydro)cerussite, and thus sheds new light on the whitening of red lead [38].

By reducing the beam size to a few tens of a nanometre, the number of crystals and of orientations diffracting in the probed volume decreases, and in some cases, powder diffraction condition may no longer be fulfilled, and azimuthal distribution of ring intensities is no longer uniform. Besides, few grains in the proper orientation may give a strong diffracted beam, saturating the detector and usually requiring reducing the counting time. In this case, azimuthal integration of the signal can become unreliable, and the quantitative analysis can be extremely challenging. To preserve the lateral resolution, but increase the number of diffracting crystals, one solution consists in increasing the spectral range of the primary beam,

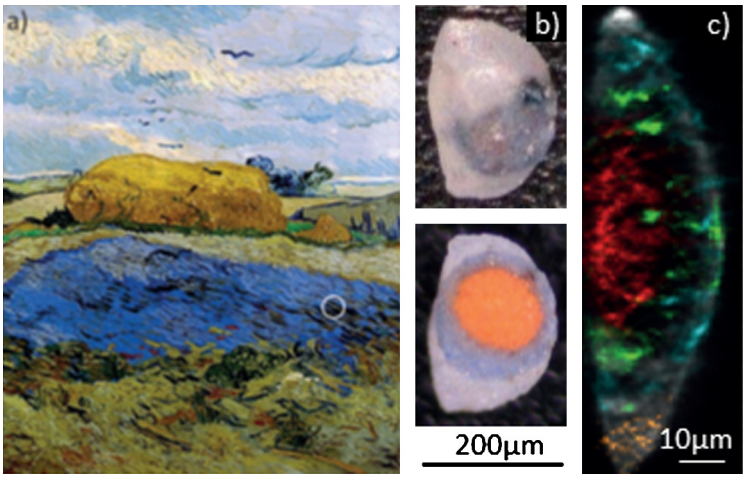


**Fig. 3.** (a) Haystacks, V. Van Gogh, Kroeller–Mueller Museum, Otterlo, NL; (b) exterior (top) and interior (bottom) view of the protrusion, showing a central part containing minium, surrounded by two white/blueish layers containing lead white; (c) XRPD 2D tomographic maps of minium (red), plumbonacrite (green), hydrocerussite (white), cerussite (light blue), and zinc white (orange). (From [38].)

using a pink, or in an extreme case, a white beam. The development of the so-called Laue micro-X-ray diffraction was made possible thanks to the development of high-brightness synchrotron sources, high-efficiency achromatic X-ray focusing optics and advanced computational indexation algorithms [39]. This technique also benefits from a higher flux, offering faster acquisitions than in monochromatic mode. It can also provide information about grain orientation. It has already been successfully applied to determine the mineralogy of colour pigments taken from the ancient Egyptian coffin of Tjeseb, a priestess of the Apis bull dating from the third intermediate to late period, 25th Dynasty to early 26th Dynasty (747 to 600 BC) [39]. The same technique was used to investigate the micro-structural morphology of Chinese purple, in order to assess similarities and differences in the processes for making this pigment and for Egyptian blue [40]. The advantages of a hybrid approach combining micro-XRD in white-beam and in monochromatic conditions for the characterization of ancient materials are reviewed with three other examples, Roman terra sigillata, Neolithic flints, and Roman nails [41]. All these experiments were carried out at the Advanced Light Source (beamlines 7.3.3 and 12.3.2), using a micrometric beam (from 0.8 to 1.2 µm, the beam being usually bigger, ∼10 µm, for monochromatic beam, in order to increase the flux). It is clear that this technique performed with a nano-probe can have many applications in the field of cultural heritage.

### *3.3. Speciation characterization at the nano scale: nano-XAS*

#### *3.3.1. Hard X-ray nano-XAS analysis*

As an alternative or complementarily to XRD, XAS is increasingly used to get insight into matter composition in artistic objects. This family of techniques consists in measuring the variation of the X-ray absorption coefficient, while scanning the energy of the incoming beam, below and above the edge of a particular element. The absorption can be measured directly (in transmission mode), or indirectly (through the measurement of fluorescence or total electron yield). In X-ray absorption near-edge spectroscopy (XANES), the absorption is measured in a restricted energy range of ∼100 eV across the absorption edge and reflects a variation in the excitation cross section of the core electrons into unoccupied states or into the vacuum continuum. This technique probes the molecular environment of the element of interest (oxidation state, coordination number, site symmetry, and distortion). With extended X-ray absorption fine structure (EXAFS), the energy range is extended far beyond the absorption edge of interest (500–1000 eV). EXAFS oscillations result from constructive and destructive interferences between the forward propagating and the photoelectron waves backscattered by surrounding atoms. Modelling EXAFS oscillations give access to the identity of these surrounding atoms, bond distances, and coordination numbers.

Applications of XAS techniques in the field of cultural heritage are many and have been recently reviewed [5,42,43]. The possibility to discriminate species, even in complex matrices and without constraints with respect to the crystallinity of compounds, is a real asset. It explains why it is widely used to analyse amorphous materials such as glasses and glazes. XAS can be applied with a relatively large beam to follow in real time the speciation of an element in a dynamic system. This approach can be used to investigate electrochemical or photochemical degradation processes, mimicking corrosion or photo alteration of artistic matter. As an example, time-resolved Fe K-edge XANES has been employed to follow Fe redox processes during Prussian blue discolouration and to assess more particularly the effect of substrate content, structure, and photosensitivity as well as oxygen environment [44]. In such a case, the sample is considered as homogeneous. More particularly here, the sample (a 0.5 × 0.5-$cm^2$ piece of cellulosic paper immersed in a Prussian blue solution) was moved horizontally and vertically under a 35-µm beam during acquisition to smooth the heterogeneous distribution of pigment particles in fibres.

Alternatively, when the samples exhibit a strong heterogeneity, μXAS can be used to precisely identify and localize the different species. This is particularly interesting when the same element can be present under different speciations, as a result of chemical reactions involved in the production of artistic matter and/or during degradation processes as well. As an example, Sb $L_1$-edge μXANES was performed with a sub-micrometric beam to determine Sb speciation specifically in the glass matrix and in calcium antimonate crystals in a collection of Egyptian, Roman, and French opaque glasses [45–47]. This technique proved to be very efficient to discriminate an *in situ* production of calcium antimonate nano-crystals (by reaction of antimonate oxides with the Ca present in the glass matrix), from an *ex-situ* production of the crystals (by the addition in the glass of a calcium antimonate powder). μXANES is also extensively used to study degradation processes, for instance corrosion of aluminium in air and space museum aircrafts [48], or degradation and migration of orpiment, realgar, and emerald green pigments in historical paintings [49,50]. The first step of such micro-analyses usually consists in acquiring μXRF elemental maps to check the distribution of the element of interest and to assess its possible co-localization with other elements. In a second step, μXANES spectra are acquired over a few points of interest, to reveal locally the composition of the matter. Possibly, these analyses can be completed by the acquisition of qualitative and, in some cases, quantitative speciation maps: it consists in acquiring few μXRF maps at few peculiar energies, those giving the highest contrast between the compounds hypothetically present in the sample [51]. Using XANES spectra of reference materials, these μXRF maps can be converted into valence state maps. When applicable, this approach is very efficient to reveal the distribution of different species over large regions. Degradation layers usually form at the surface of objects and can develop over a few microns. Accordingly, the use of a micrometric beam is requested to specifically probe the degraded area and to compare the spectral signal with the one acquired in inner, unaged matter. However, in some cases, zooming further into the matter may be necessary to obtain a more detailed localization of the different constituents. As an example, As K-edge nano-XANES has been used at the ID16B beamline, ESRF, to study the degradation of As-based pigments in paint micro-samples from Baroque- and Rococo-era paintings [52]. Orpiment and realgar, both arsenic sulphide pigments respectively used for their vivid yellow and red–orange hues, can quickly degrade to arsenic trioxide and arsenate. This often results in whitening or transparency in the painted surfaces. While conventional techniques such as microscopic Raman and μFTIR spectroscopies can allow a quick and relatively easy identification of the orpiment, realgar, artificial arsenic sulphide glass and, to some extent, arsenic oxide, the identification and visualization of distributions of the degradation products – and especially arsenate compounds – in the paint micro-samples is generally more challenging. In this study, SR nano-XRF mapping was performed using a $100 \times 100$ nm$^2$ produced with a KB mirror system. The analysis carried out on a visually degraded orpiment-containing paint stratigraphy, originating from a 17th-century painting, revealed that arsenic is distributed throughout the entire cross-section, while nano-XANES demonstrated that arsenic is present in both arsenite (As-III) and arsenate (As-V) forms [52]. To obtain oxidation-state specific maps of As, As XRF distributions at three primary energies were recorded: $En_1 = 11.869$ keV (only arsenides excited), $En_2 = 11.874$ keV (predominantly arsenates excited), and $En_3 = 11.920$ keV (post edge, all As species excited). The total arsenic distribution map ($\Sigma$As, $En_3$) (Fig. 4c) showed that arsenic species are present at various concentration levels throughout the sample. The As(-II)/$\Sigma$As ratio map (labelled RG in Fig. 4c), normalized to the total As content, allowed us to visualize the arsenic sulphide pigment particles present in the paint layer (red channel) and the distribution of the arsenate (green channel) in relation to these. When comparing the $En_1$ and $En_2$ maps in Fig. 4c, a slight gradient can be observed when going from the core to the shell of the pigment particle, whereas a more important presence of arsenate is observed around the pigment particles. The wide spread of arsenates observed could be explained either as a result of a migration of the degraded arsenate compound(s) through the layer using the internal moisture of the paint layers as a carrier, as suggested by Keune et al. [50], or could be interpreted as being the result of the complete oxidation of very fine pigment particles. During the investigation, the combination of nano-XRF and nano-XANES was very useful for the characterization of the advanced degradation state of the arsenic-containing pigments in paint systems. This type of information could not be obtained by means of conventional spectroscopic methods of microanalysis such as Raman microscopy.

*3.3.2. Soft X-ray nano-XAS analysis*

While the development of nano-XAS in the hard X-ray range (>5 keV) is rather recent, its equivalent in the soft X-ray range (usually called NEXAFS for near-edge X-Ray absorption fine structure) has been used for decades. This is thanks to the fact that focusing X-ray beam below 100 nm was made possible much earlier in the soft X-ray range than in the hard X-ray range. As detailed in [53], a sequence of X-ray absorption images is acquired at closely spaced photon energies using a scanning transmission X-ray microscope (STXM), and aligned. NEXAFS spectra are then obtained both from large, irregular regions, and from regions as small as the spatial resolution of the microscope (about 40 nm in the examples shown in this pioneering publication). By rotating the sample, this technique can even be extended to 3D [54]. Applications to ancient materials were first in the field of natural heritage (palaeontology, paleo-environment). As an example, STXM at the carbon K-edge can be used to identify major organic functional groups, even in strongly diagenetized biological systems [55]. Applications to cultural heritage are still few but will certainly increase in the future. It could be used not only at the K-edge of low-$Z$ elements such as C, O, N, but also at the L-edges of heavier elements, such as metals. For instance, STXM has been used at the Fe L-edges to study corrosion mechanisms in ferrous artefacts with a nano-probe of about 25 nm [56]. More recently, a combination of NEXAFS at the C K-edge and Fe $L_{2,3}$ edges was used to investigate the penetration of iron gall ink in paper fibres [57]. The former showed slight spectral differences between primary cell wall and secondary cell wall in the linen fibres. It highlighted as well the distribution of gallic acid and gum arabic, introduced in ink. The latter

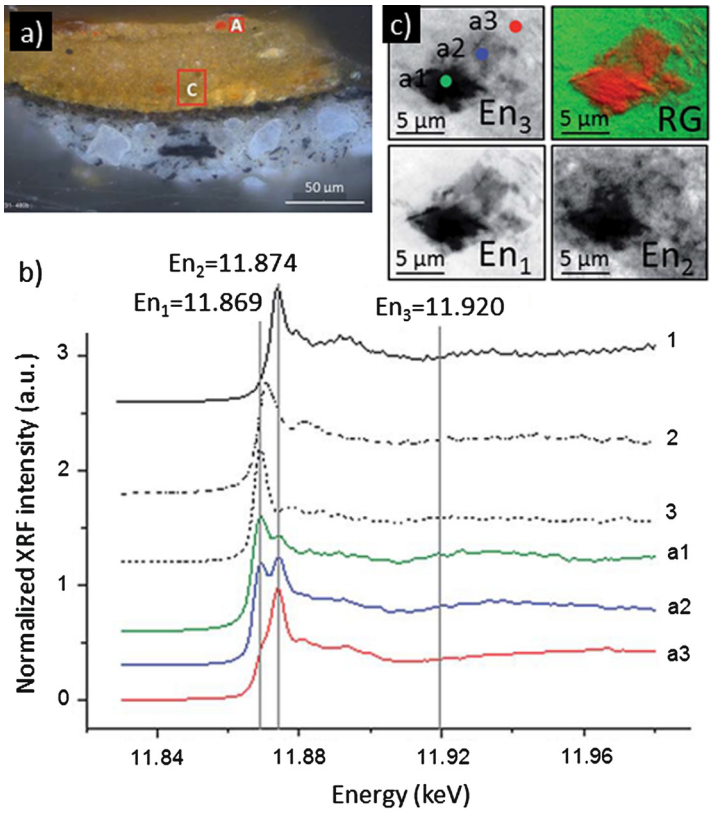


**Fig. 4.** (a) Optical micrograph of orpiment-containing paint layer from a 17th-century painting. The rectangles A and C represent two regions where nano-XRF and nano-XAS analyses were performed. (b) As-K edge XANES spectra (a1–a3) from a degraded grain as orpiment ($As_2S_3$) in this sample, in region A and from reference compounds (1: $K_3AsO_4$; 2: $As_2O_3$; 3: $As_2S_3$). Peaks corresponding to arsenides (at $En_1$) and arsenates (at $En_2$) are visible. (c) As-XRF maps recorded over the region A at three different energies, indicated in (b). $En_3$ was used to record the distribution of the totality of As species present. The ratio map (RG) shows the arsenide-to-total arsenic intensity (red: high ratio, indicating the predominant presence of arsenides; green: low ratio, corresponding to the predominant presence of arsenates). (From [52].)

revealed the penetration of iron in ink fibres, and an uneven migration and distribution of Fe(II) vs. Fe(III). Such observations with a resolution of a few tens of nanometres provide unique information about ink penetration in paper fibres and could be further exploited to study the role of ink in the degradation of manuscripts.

### *3.3.3. XAS-full-field transmission X-ray microscopy analysis*

Finally, X-ray speciation maps can be obtained with a nanometric resolution, but without a nanometric beam. This can be done using full-field transmission X-ray microscopy (TXM). In this technique, the sample does not need to be scanned. Instead, X-ray radiographies are acquired using a 2D detector. In a similar fashion to STXM, the acquisition of radiographies while sequentially tuning the energy of the incoming X-ray beam provides XAS spectra over a 2D surface, or even a 3D volume, if the sample is further rotated. Resolution of a few tens of nanometres can be obtained, while preserving fields of view of few tens or hundreds of microns. As an example, this technique has been used to identify and map iron species in cross-sections of Roman and Greek ceramics, in the different parts of the structure (red/black gloss, body) and substructure (within these layers) [58,59]. XANES data were correlated with porosity (obtained by X-ray tomography). The results could be related to manufacturing processes and in particular red/ox and temperature conditions in the different steps of the firing process.

## *3.4. Other non-X-ray based spectro/imaging techniques*

Even if this review is dedicated to synchrotron-based nano-probes, it is important to mention that other laboratory techniques can provide chemical mapping with nanometric resolution [60]. The most common techniques used to study fragments from artefacts are probably those based on electron nano-probes. In particular, transmission electron microscopy (TEM), possibly combined with an energy-dispersive spectrometer (EDS), as well as electron energy loss spectroscopy (EELS), respectively, provide structural, elemental, and speciation characterization with resolution in the range of the nanometre. They have been extensively used to characterize ceramics coatings, lustres, but also pigment degradation [60–62].

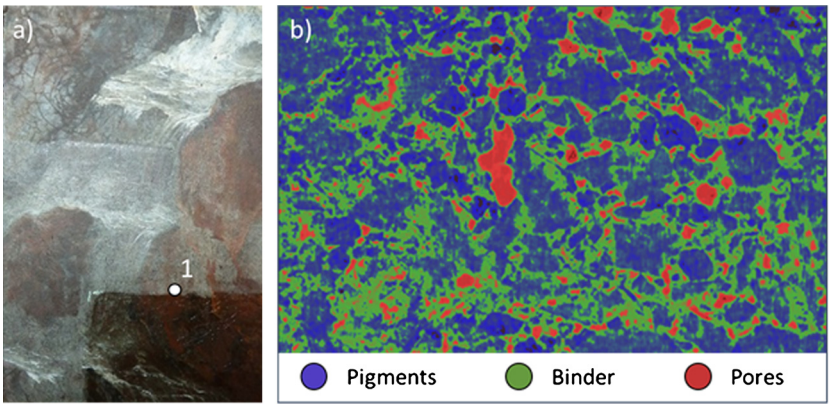


**Fig. 5.** (a) An example of blanching of paint layers in a painting of Johannes van der Bent, *Paysage, figures et animaux*, 17th century, oil on canvas, 794.1.1, "musée des Beaux-Arts", Rennes. In the darker area, the alteration was treated with an unstainable result with a DMSO/ethyl acetate (30/70) mixture and subsequent Regalrez® varnish application. © C2RMF/A. Maigret. (b) Detail of a phase-contrast nanotomography reconstructed slice of sample 1, highlighting the presence of pores in the organic binder.

Infrared spectroscopy is commonly used to characterize artistic materials [63]. Infrared microscopes are particularly efficient for the study of heterogeneous fragments [64]. About 15 years ago, the development of synchrotron-based infrared microscopes gave access to lateral resolution of a few microns [65]. Today, many efforts are dedicated to the development of nano-infrared instruments, being with laser or synchrotron sources, giving access to resolutions of a few tens of nanometres. First applications to cultural heritage have already been reported (e.g., for the characterization of collagen degradation in altered parchments [66]). A resolution of ∼50–100 nm is obtained by using a sharp tip, which serves as a near-field detector and locally detects the small thermal expansion due to the absorption of infrared light by the sample. Similarly, tip enhanced Raman spectroscopy (TERS) allows the acquisition of Raman spectra with a nanometric resolution and was used to identify indigo dye and iron gall ink on papers [67].

Ion nano-probes also find various applications in the field of cultural heritage. Time-of-flight secondary ion mass spectrometry (ToF-SIMS) and nano-SIMS provide chemical and isotopic mapping, with a resolution of ∼200 down to ∼50 nm, respectively. In a similar fashion to infrared microscopy, these techniques are very efficient for the study of artistic materials, in particular painting, since they simultaneously probe organic and inorganic compounds [68,69].

### *3.5. Morphological characterization at the nano scale by X-ray phase contrast computed tomography*

In parallel to the determination of elemental, structural, and chemical composition, SR-based imaging techniques are also widely used to obtain the 3D characterization of the morphology of the samples. SR phase-contrast micro-computed tomography (μCT) is a very efficient technique to reveal the inner micro/nano structure of materials. It is regularly used to scan paleontological specimens [70], but applications to artistic materials have also been reported, in particular for the study of iron corroded rebars [71] or paint fragments [72–74]. In such cases, the aim is usually to determine the presence, size, and distribution of corrosion products, pigment particles or pores over 3D volumes.

For this technique as well, efforts are made to further improve spatial resolution. The use of a divergent beam focused by Kirkpatrick–Baez mirrors, instead of a parallel geometry, enables to access nowadays lower spatial resolutions, thanks to a geometric demagnification of the source size. Synchrotron beamlines such as ID16A at the ESRF reach resolution down to 25 nm [75]. Contrary to absorption tomography, the use of phase-contrast nanotomography (or nano-holotomography) enables to distinguish regions with low and similar electron densities (organic matter, pores) in the presence of high-density compounds (iron, copper, lead…). This technique is thus particularly relevant for cultural heritage artefacts that are highly heterogeneous. At the ID16A beamline, phase contrast nanotomography is performed by recording four tomographic scans in full field mode, by putting the detector at four near-field propagation distances (Fresnel domain). It gives both a large field of view ($51 \times 51 \times 51\ \mu m^3$) and a high spatial resolution (25 nm). Three dimensional images are then obtained from retrieved phase maps by tomographic reconstruction. As an example, X-ray phase contrast nanotomography was recently used to investigate the blanching of oil paintings, a frequent alteration induced by an excessive humidity (Fig. 5a). It can affect varnish and paint layers, strongly altering their visual appearance. FEG-SEM examinations revealed a highly porous structure in altered layers, with pores ranging in size from a few nanometres to a few micrometres [76]. The presence of mainly submicronic pores induces a strong light scattering and therefore a degradation of the visual appearance [77]. Regarding the blanching of paint layer, phase contrast nanotomography analyses highlighted that pores are located in the binder, which revealed that the degradation takes place in the organic matter (Fig. 5b). Moreover, it shows that current conservation treatments are not efficient to durably fill the pores or resorb them. These results have constituted a major advance towards the characterization of the alteration and provided interesting perspectives concerning its understanding and the proposal of adapted and durable conservation treatments [78].

## 4. Challenges associated with the use of nano-probes

The transition from macro to micro and even nano-analyses not only requires the development of instruments (in particular of focusing optics), but necessitates as well the careful consideration of additional experimental factors, along the entire analytical chain, from sample preparation to data acquisition and data processing.

### *4.1. Issues with sample preparation*

In the field of cultural heritage, the most standard sample preparation consists in embedding the sample in resin and polishing one surface to reveal the sample's stratigraphy. This preparation is highly suitable for optical light microscopy or scanning electron microscopy. It can also be used for μXRF, μXAS measured in μXRF mode [45–47], and μXRD if the X-ray penetration is sufficient (embedded sample sufficiently small and/or energy sufficiently high). At 10 keV, the X-ray penetration depth is typically a few tens of microns over common artistic materials. It means that when the beam is focused to a few tens of nanometres, the analysed volume is strongly asymmetric, with an in-depth resolution possibly 2000 times larger than the lateral resolution. This means that the signal that is collected (in particular in XRF mode) does not necessarily reflect the composition of the visible surface [28]. In some cases, this high penetration can be exploited to obtain 3D acquisitions, as illustrated above by the 3D XRPD analysis of a protrusion in a Van Gogh painting [38] (or the holotomography of blanching paint [78]). However, such 3D analyses are more time consuming than their equivalent 2D analyses, more demanding from a data processing point of view and impose to work at sufficiently high energies (not necessarily compatible with XAS analyses). Alternatively, the issue of high penetration depths can be circumvented by preparing thin sections [79]. This allows the precise control of the analysed depth. The thickness will depend on the energy of the incoming X-ray beam. For STXM analyses (in the soft X-ray range), focused ion beam (FIB) sections of a few tens of nanometres are usually prepared and deposited on TEM grids [55–57]. For analyses in the hard X-ray range, thin sections of a few microns are generally more suitable. They can be obtained using a microtome, in particular for soft materials such as paintings [31,80] or by double-side polishing, for harder materials, such as ceramics [58,59].

### *4.2. Issues with data acquisition*

While reducing the beam size, acquisitions are more and more sensitive to any beam motion. These motions can be due to electron beam motion, thermal variations on the optics, mechanical instabilities, etc. In particular, keeping fixed a nano-beam during XAS acquisitions (meaning while scanning the monochromator's crystals) is a real challenge. In parallel to the development of state-of-the-art monochromators, other strategies are followed to correct for the beam motion. One of them consists in hypothesizing that the beam motion is reproducible over a certain energy range and can be recorded in a table. The sample position is then corrected synchronously with the beam energy using this table [26]. Ideally, such a correction should be done in real time over continuous scans. Alternatively, another strategy for the acquisition of nano-XAS data consists in acquiring hyperspectral 2D XRF maps. Even if maps are shifted from one energy to another, this motion can be corrected afterwards, and the images aligned [53,81]. At ID21, ESRF, a software has been developed to make this correction on-line, during acquisitions. This strategy allows not only the acquisition of XAS spectra on nano-objects, but also provides a 2D spectral characterization of the samples [82].

Whatever the technique, the smaller the gauge volume, the less representative the measurement might become. Accordingly, it is important to keep the field of view sufficiently large to preserve the representativeness of the measurements. Therefore, when efforts are made to decrease the beam, others should be made to increase the acquisition speed to preserve the representativeness of the measurements. Improving the sample resolution by a factor 10 (e.g., from 1 μm to 100 nm) implies that the acquisition of the same 2D map, preserving the same pixel dwell time and same field of view, requires 100 more time (e.g., 17 h instead of 10 min). In this respect, the development of ultra-fast detectors is a must. As an example, the assets offered by the so-called MAIA detector have been well illustrated by the full spectral XANES imaging of the degradation of chrome yellow pigments in some Van Gogh paintings [83]. Besides, a hierarchical approach with progressive analyses at the millimetric, micrometric, and nanometric scales is essential to ensure the representativeness of the results.

Concentrating the same number of photons in a nano-probe instead of a micro-probe implies that the dose increases. This means that, at constant flux, radiation damage risk and impact will be higher during nano-analyses. Of course, one solution to reduce the dose consists in shifting the sample slightly out of the focal point, to spread to photons over a larger surface. However, this is counterproductive with respect to the use of a nano-probe. Instead, other mitigation strategies should be followed, such as avoidance of unnecessary beam exposure, improvement of detection efficiency and data collection (e.g., continuous scans), reduction of the flux by using attenuators, optimization of the sample environment [83]. Monitoring and recording strategies to evaluate the impact of the beam on the sample should also be carefully considered [83]. In the field of biology and in particular protein crystallography, maintaining the sample in cryo-conditions is a standard method to reduce radiation damage. This strategy is rarely applied to samples from artefacts (possibly due to the sample preciousness and the physical risks associated with cooling samples), but this strategy should be further considered in the future, in particular at nano-beamlines. Tests could be first carried out on model samples.

### 4.3. Issues with data processing and data analysis

The use of nano-probe poses a certain number of problems for data processing and data analysis. As mentioned above, the risk of radiation damage and accordingly of misinterpretation of data, in particular nanoXAS and nanoXRPD results, increase while focusing the beam in a smaller probe, and must be carefully considered, monitored, and mitigated as much as possible.

Concerning XRF, while one could think that XRF quantification methods traditionally used on micro-probes can be easily extended to nano-probes, pioneer experiments at the new nano-probe beamline ID16B, ESRF, showed that this is not the case and that quantification XRF mapping of metal traces in solid samples requires specific efforts, in particular in terms of sample preparation and reference preparation [84]. In addition to the control of the thickness, it is recommended to minimize as well the size of the sample laterally (to reduce the contribution of XRF from regions out of the volume of interest, which would be excited by the lateral wings of the beam profile).

Besides, when the beam size is in the range or below the size of the crystallites, orientation effects may affect the data (e.g., polarisation effect in nano-XAS; diffraction patterns no longer in Debye–Scherrer conditions, as mentioned in Section 3.2) impacting data interpretation and quantitative treatment.

To evaluate all these risks (damage, orientation…) and their impact on data, the “zoom-in” strategy can help as well. Preliminary analyses can be carried on homogeneous model samples mimicking the composition of historical samples. Data obtained with a nano-probe can be confronted to millimetric measurements. Any discrepancy between the two sets of measurements can be primarily ascribed to artefacts related to the probe size itself and should be understood, limited (by adapting sample preparation, data acquisition, data processing…) and quantified before analysing heterogeneous historical samples.

## 5. Conclusion

The use of SR-based nano-probes in the field of cultural heritage is still limited, however increasing. They offer a further zoom in the artistic matter and give the possibility to identify and precisely localize the different components constitutive of the matter, with two main deliverables: (i) the selective characterization of the composition of sub-micrometric objects (e.g., pigment nanoparticles); (ii) the precise determination of the composition at the interface between constituents (to track the presence and distribution of degradation products in very thin alteration layers, or of pores in binders, etc.). The variety of techniques, already commonly used with macro- and micro-beams at synchrotron facilities (XRF, XRD, XAS, FTIR, CT), allows one to tackle the matter under different complementary points of view. A few more challenges must be carefully considered in the transition from micro- to nano-analyses (not only in the focalization of the beam itself, but also in sample preparation, data acquisition, data analysis, and interpretation). However, zooming-in further into the heterogeneity of artistic matter and discovering more about the information entrapped in this matter is well worth the effort.

## References

[1] L. Bertrand, et al., Development and trends in synchrotron studies of ancient and historical materials, Phys. Rep. 519 (2) (2012) 51–96.
[2] L. Bertrand, M. Thoury, E. Anheim, Ancient materials specificities for their synchrotron examination and insights into their epistemological implications, J. Cult. Heritage 14 (4) (2013) 277–289.
[3] L. Bertrand, et al., Emerging approaches in synchrotron studies of materials from cultural and natural history collections, Top. Curr. Chem. 374 (1) (2016) 7.
[4] K. Janssens, et al., Non-invasive and non-destructive examination of artistic pigments, paints, and paintings by means of X-ray methods, Top. Curr. Chem. 374 (6) (2016) 81.
[5] M. Cotte, et al., Synchrotron-based X-ray absorption spectroscopy for art conservation: looking back and looking forwards, Acc. Chem. Res. 43 (6) (2010) 705–714.
[6] M. Alfeld, et al., A mobile instrument for in situ scanning macro-XRF investigation of historical paintings, J. Anal. At. Spectrom. 28 (5) (2013) 760–767.
[7] J. Dik, et al., Visualization of a lost painting by Vincent van Gogh visualized by synchrotron radiation based X-ray fluorescence elemental mapping, Anal. Chem. 80 (2008) 6436–6442.
[8] W. De Nolf, et al., High energy X-ray powder diffraction for the imaging of (hidden) paintings, J. Anal. At. Spectrom. 26 (5) (2011) 910–916.
[9] F. Vanmeert, et al., Highly-specific chemical mapping by macroscopic X-ray powder diffraction (MA-XRPD) of Van Gogh's Sunflowers allows to identify areas with higher degradation risk, Angew. Chem. Int. Ed. 25 (2018) 7418–7422.
[10] G.E. Ice, J.D. Budai, J.W. Pang, The race to x-ray microbeam and nanobeam science, Science 334 (6060) (2011) 1234–1239.
[11] K. Yamauchi, et al., Figuring with subnanometer-level accuracy by numerically controlled elastic emission machining, Rev. Sci. Instrum. 73 (11) (2002) 4028–4033.
[12] H. Mimura, et al., Breaking the 10 nm barrier in hard-X-ray focusing, Nat. Phys. 6 (2) (2010) 122.
[13] J.C. Da Silva, et al., Efficient concentration of high-energy x-rays for diffraction-limited imaging resolution, Optica 4 (5) (2017) 492–495.
[14] A. Snigirev, et al., A compound refractive lens for focusing high-energy X-rays, Nature 384 (6604) (1996) 49.
[15] J. Vila-Comamala, et al., Zone-doubled Fresnel zone plates for high-resolution hard X-ray full-field transmission microscopy, J. Synchrotron Radiat. 19 (5) (2012) 705–709.
[16] E. Di Fabrizio, et al., High-efficiency multilevel zone plates for keV X-rays, Nature 401 (6756) (1999) 895.
[17] H. Kang, et al., Nanometer linear focusing of hard x rays by a multilayer Laue lens, Phys. Rev. Lett. 96 (12) (2006) 127401.
[18] H.C. Kang, et al., Focusing of hard x-rays to 16 nanometers with a multilayer Laue lens, Appl. Phys. Lett. 92 (22) (2008) 221114.
[19] E. Nazaretski, et al., Performance and characterization of the prototype nm-scale spatial resolution scanning multilayer Laue lenses microscope, Rev. Sci. Instrum. 84 (3) (2013) 033701.
[20] M. Schreiner, M. Melcher, K. Uhlir, Scanning electron microscopy and energy dispersive analysis: applications in the field of cultural heritage, Anal. Bioanal. Chem. 387 (3) (2007) 737–747.

[21] A.N. Shugar, J.L. Mass, Handheld XRF for Art and Archaeology, vol. 3, Leuven University Press, Leuven, Belgium, 2012.
[22] K. Janssens, et al., Use of microscopic XRF for non-destructive analysis in art and archaeometry, X-Ray Spectrom. 29 (1) (2000) 73–91.
[23] M. Alfeld, et al., Visualizing the 17th century underpainting in Portrait of an Old Man by Rembrandt van Rijn using synchrotron-based scanning macro-XRF, Appl. Phys. A 111 (1) (2013) 157–164.
[24] E. Brun, et al., Revealing metallic ink in Herculaneum papyri, Proc. Natl. Acad. Sci. 113 (14) (2016) 3751–3754.
[25] M. Cotte, et al., Applications of synchrotron-based micro-imaging techniques to the chemical analysis of ancient paintings, J. Anal. At. Spectrom. 23 (2008) 820–828.
[26] M. Cotte, et al., Synchrotron-based X-ray spectromicroscopy used for the study of an atypical micrometric pigment in 16th century paintings, Anal. Chem. 79 (2007) 6988–6994.
[27] S. Cersoy, et al., Identifying and quantifying amorphous and crystalline content in complex powdered samples: application to archaeological carbon blacks, J. Appl. Crystallogr. 49 (2) (2016) 585–593.
[28] F. Casadio, V. Rose, High-resolution fluorescence mapping of impurities in historical zinc oxide pigments: hard X-ray nanoprobe applications to the paints of Pablo Picasso, Appl. Phys. A 111 (1) (2013) 1–8.
[29] R.P. Winarski, et al., A hard X-ray nanoprobe beamline for nanoscale microscopy, J. Synchrotron Radiat. 19 (6) (2012) 1056–1060.
[30] T. Ungár, et al., Revealing the powdering methods of black makeup in ancient Egypt by fitting microstructure based Fourier coefficients to the whole x-ray diffraction profiles of galena, J. Appl. Phys. 91 (4) (2002) 2455–2465.
[31] V. Gonzalez, et al., Synchrotron-based high angle resolution and high lateral resolution X-ray diffraction: revealing lead white pigment qualities in old masters paintings, Anal. Chem. 89 (24) (2017) 13203–13211.
[32] L. Monico, et al., The degradation process of lead chromate in paintings by Vincent van Gogh studied by means of spectromicroscopic methods. Part III: Synthesis, characterization and detection of different crystal forms of the chrome yellow pigment, Anal. Chem. 85 (2) (2013) 851–859.
[33] L. Monico, et al., The degradation process of lead chromate in paintings by Vincent van Gogh studied by means of spectromicroscopic methods. Part IV: Artificial ageing of model samples of co-precipitates of lead chromate and lead sulfate, Anal. Chem. 85 (2) (2013) 860–867.
[34] M. Radepont, et al., Thermodynamic and experimental study of the degradation of the red pigment mercury sulfide, J. Anal. At. Spectrom. 30 (3) (2015) 599–612.
[35] F. Da Pieve, et al., Casting light on the darkening of colors in historical paintings, Phys. Rev. Lett. 111 (20) (2013) 208302.
[36] W. Anaf, K. Janssens, K. De Wael, Formation of metallic mercury during photodegradation/photodarkening of $\alpha$-HgS: electrochemical evidence, Angew. Chem. 125 (48) (2013) 12800–12803.
[37] P. Bleuet, et al., Probing the structure of heterogeneous diluted materials by diffraction tomography, Nat. Mater. 7 (6) (2008) 468–472.
[38] F. Vanmeert, G. Van der Snickt, K. Janssens, Plumbonacrite identified by X-ray powder diffraction tomography as a missing link during degradation of red lead in a Van Gogh painting, Angew. Chem. 54 (12) (2015) 3678–3681.
[39] P.A. Lynch, et al., Application of white-beam X-ray microdiffraction for the study of mineralogical phase identification in ancient Egyptian pigments, J. Appl. Crystallogr. 40 (6) (2007) 1089–1096.
[40] Z. Liu, et al., Influence of Taoism on the invention of the purple pigment used on the Qin terracotta warriors, J. Archaeol. Sci. 34 (11) (2007) 1878–1883.
[41] C. Dejoie, et al., Complementary use of monochromatic and white-beam X-ray micro-diffraction for the investigation of ancient materials, J. Appl. Crystallogr. 48 (5) (2015) 1522–1533.
[42] F. Farges, M. Cotte, X-ray absorption spectroscopy and cultural heritage: highlights and perspectives, in: J.A. Van Bokhoven, C. Lamberti (Eds.), X-Ray Absorption and X-Ray Emission Spectroscopy: Theory and Applications, John Wiley & Sons, Chichester, UK, 2016, pp. 609–636.
[43] K. Janssens, M. Cotte, The use of XAS and related methods in Cultural Heritage investigations, International Tables for Crystallography, vol. I, ch. 8.16, in press.
[44] C. Gervais, et al., Time resolved XANES illustrates a substrate-mediated redox process in Prussian blue cultural heritage materials, J. Phys. Conf. Ser. (2016).
[45] S. Lahlil, et al., Synthesis of calcium antimonate nano-crystals by the 18th dynasty Egyptian glassmakers, Appl. Phys. A 98 (1) (2010) 1–8.
[46] S. Lahlil, et al., New insight on the in situ crystallization of calcium antimonate opacified glass during the Roman period, Appl. Phys. A 100 (3) (2010) 683–692.
[47] S. Lahlil, et al., Synthesizing lead antimonate in ancient and modern opaque glass, J. Anal. At. Spectrom. 26 (5) (2011) 1040–1050.
[48] F. Mirambet, et al., Synchrotron radiation contribution to the study of aluminium corrosion layers of air and space museum aircrafts for their preservation, J. Anal. At. Spectrom. 31 (8) (2016) 1631–1637.
[49] K. Keune, et al., Analytical imaging studies of the migration of degraded orpiment, realgar, and emerald green pigments in historic paintings and related conservation issues, Heritage Sci. 4 (1) (2016) 10.
[50] K. Keune, et al., Tracking the transformation and transport of arsenic sulfide pigments in paints: synchrotron-based X-ray micro-analyses, J. Anal. At. Spectrom. 30 (3) (2015) 813–827.
[51] G. Nuyts, et al., Micro-XANES study on Mn browning: use of quantitative valence state maps, J. Anal. At. Spectrom. 30 (3) (2015) 642–650.
[52] M. Vermeulen, et al., Visualization of As(III) and As(V) distributions in degraded paint micro-samples from Baroque- and Rococo-era paintings, J. Anal. At. Spectrom. 31 (9) (2016) 1913–1921.
[53] Jacobsen, et al., Soft X-ray spectroscopy from image sequences with sub-100 nm spatial resolution, J. Microsc. 197 (2) (2000) 173–184.
[54] M. Obst, G. Schmid, 3D chemical mapping: application of scanning transmission (soft) X-ray microscopy (STXM) in combination with angle-scan tomography in bio-, geo-, and environmental sciences, in: J. Kuo (Ed.), Electron Microscopy: Methods and Protocols, Humana Press, Totowa, NJ, USA, 2014, pp. 757–781.
[55] S. Bernard, et al., Ultrastructural and chemical study of modern and fossil sporoderms by scanning transmission X-ray microscopy (STXM), Rev. Palaeobot. Palynol. 156 (1) (2009) 248–261.
[56] A. Michelin, et al., Investigation at the nanometre scale on the corrosion mechanisms of archaeological ferrous artefacts by STXM, J. Anal. At. Spectrom. 28 (1) (2013) 59–66.
[57] V. Rouchon, S. Bernard, Mapping iron gall ink penetration within paper fibres using scanning transmission X-ray microscopy, J. Anal. At. Spectrom. 30 (3) (2015) 635–641.
[58] F. Meirer, et al., Full-field XANES analysis of Roman ceramics to estimate firing conditions—a novel probe to study hierarchical heterogeneous materials, J. Anal. At. Spectrom. 28 (12) (2013) 1870–1883.
[59] I. Cianchetta, et al., Evidence for an unorthodox firing sequence employed by the Berlin painter: deciphering ancient ceramic firing conditions through high-resolution material characterization and replication, J. Anal. At. Spectrom. 30 (2015) 666–676.
[60] P. Dillmann, L. Bellot-Gurlet, I. Nenner, Nanoscience and Cultural Heritage, Springer, 2016.
[61] F. Casadio, et al., Electron energy loss spectroscopy elucidates the elusive darkening of zinc potassium chromate in Georges Seurat's A Sunday on La Grande Jatte—1884, Anal. Bioanal. Chem. (2010) 1–12.
[62] H. Tan, et al., Nanoscale investigation of the degradation mechanism of a historical chrome yellow paint by quantitative electron energy loss spectroscopy mapping of chromium species, Angew. Chem. Int. Ed. 52 (43) (2013) 11360–11363.
[63] M. Derrick, D. Stulik, J.M. Landry, Infrared spectroscopy in conservation science, in: Scientific Tools for Conservation, The Guetty Conservation Institute, Los Angeles, 1999, p. 235.

[64] S. Prati, et al., New frontiers in application of FTIR microscopy for characterization of cultural heritage materials, Top. Curr. Chem. 374 (3) (2016) 26.
[65] M. Cotte, et al., Recent applications and current trends in cultural heritage science using synchrotron-based Fourier transform infrared micro-spectroscopy, C. R. Physique 10 (7) (2009) 590–600.
[66] G. Latour, et al., Correlative nonlinear optical microscopy and infrared nanoscopy reveals collagen degradation in altered parchments, Sci. Rep. 6 (2016) 26344.
[67] D. Kurouski, et al., Tip-enhanced Raman spectroscopy (TERS) for in situ identification of indigo and iron gall ink on paper, J. Am. Chem. Soc. 136 (24) (2014) 8677–8684.
[68] B. Marino, et al., Imaging Tof-SIMS and NanoSIMS studies of berite–celestite particles in grounds from paintings by van Gogh, in: e-Preservation Science, Proceedings of 2006 AIC Annual Conference, vol. 3, American Institute for Conservation of Historic & Artistic Works, 2006, pp. 41–50.
[69] J. Sanyova, et al., Unexpected materials in a Rembrandt painting characterized by high spatial resolution cluster-TOF-SIMS imaging, Anal. Chem. 83 (3) (2011) 753–760.
[70] P. Tafforeau, et al., Applications of X-ray synchrotron microtomography for non-destructive 3D studies of paleontological specimens, Appl. Phys. A 83 (2) (2006) 195–202.
[71] M. Jacot-Guillarmod, et al., Degradation mechanisms of reinforcing iron rebars in monuments: the role of multiscale porosity in the formation of corrosion products investigated by X-ray tomography, J. Anal. At. Spectrom. 30 (3) (2015) 580–587.
[72] E.S.B. Ferreira, et al., 3D synchrotron x-ray microtomography of paint samples, in: Proceedings of SPIE – The International Society for Optical Engineering, 2009.
[73] E.S.B. Ferreira, et al., Study of the mechanism of formation of calcium soaps in an early 20th century easel painting with correlative 2D and 3D microscopy, in: ICOMCC, Lisboa, 2011.
[74] C. Gervais, et al., Characterization of porosity in a 19th century painting ground by synchrotron radiation X-ray tomography, Appl. Phys. A, Mater. Sci. Process. 111 (1) (2013) 31–38.
[75] J.C.d. Silva, et al., High-energy cryo x-ray nano-imaging at the ID16A beamline of ESRF, in: SPIE Optical Engineering + Applications, SPIE, 2017.
[76] A. Genty-Vincent, et al., Blanching of paint and varnish layers in easel paintings: contribution to the understanding of the alteration, Appl. Phys. A 121 (3) (2015) 779–788.
[77] A. Genty-Vincent, et al., Four-flux model of the light scattering in porous varnish and paint layers: towards understanding the visual appearance of altered blanched easel oil paintings, Appl. Phys. A 123 (7) (2017) 473, https://doi.org/10.1007/s00339-017-1092-1.
[78] A. Genty-Vincent, et al., Blanching of paint and varnish layers: from the characterization to the development of an efficient conservation treatment, submitted for publication.
[79] E. Pouyet, et al., Thin-sections of painting fragments: opportunities for combined synchrotron-based micro-spectroscopic techniques, Heritage Sci. 3 (1) (2015) 1–16.
[80] E. Pouyet, et al., Preparation of thin-sections of painting fragments: classical and innovative strategies, Anal. Chim. Acta 822 (2014) 51–59.
[81] M. Cotte, et al., The ID21 X-ray and infrared microscopy beamline at the ESRF: status and recent applications to artistic materials, J. Anal. At. Spectrom. 32 (2017) 477–493.
[82] L. Monico, et al., Full spectral XANES imaging using the Maia detector array as a new tool for the study of the alteration process of chrome yellow pigments in paintings by Vincent van Gogh, J. Anal. At. Spectrom. 30 (3) (2015) 613–626.
[83] L. Bertrand, et al., Mitigation strategies for radiation damage in the analysis of ancient materials, TrAC, Trends Anal. Chem. 66 (2015) 128–145.
[84] L. Lemelle, et al., Analytical requirements for quantitative X-ray fluorescence nano-imaging of metal traces in solid samples, TrAC, Trends Anal. Chem. 91 (2017) 104–111.